

A. Overview of the Supplemental Document

In this supplemental material, in Section B, we first give explicitly our 6D representation for the 3D rotations. We then prove formally in Section C that the formula of the 5D representation as defined in Case 4 of Section 4.2 satisfies all of the properties of a continuous representation. Next, we discuss quaternions in more depth. We present in Section D a result that we elided from the main paper due to space limitations: that the unit quaternions are also a discontinuous representation for the 3D rotations. Then, in Section E, we show how the continuous 5D and 6D representations can interact with common discontinuous angle representations such as quaternions. Next, we visualize in Section F discontinuities that are present in some of the representations. We finally present in Section G some additional empirical results.

B. 6D Representation for the 3D Rotations

The mapping from $SO(3)$ to our 6D representation is:

$$g_{GS} \left(\left[\begin{array}{c|c|c} a_1 & a_2 & a_3 \\ \hline \end{array} \right] \right) = \left[\begin{array}{c|c} a_1 & a_2 \\ \hline \end{array} \right] \quad (14)$$

The mapping from our 6D representation to $SO(3)$ is:

$$f_{GS} \left(\left[\begin{array}{c|c} a_1 & a_2 \\ \hline \end{array} \right] \right) = \left[\begin{array}{c|c|c} b_1 & b_2 & b_3 \\ \hline \end{array} \right] \quad (15)$$

$$b_i = \left[\begin{array}{l} N(a_1) \quad \text{if } i = 1 \\ N(a_2 - (b_1 \cdot a_2)b_1) \quad \text{if } i = 2 \\ b_1 \times b_2 \quad \text{if } i = n. \end{array} \right]^T \quad (16)$$

C. Proof that Case 4 gives a Continuous Representation

Here we show that the functions f_P, g_P presented in Case 4 of Section 4.2 are a continuous representation. We now prove some properties needed to show a continuous representation: that g_P is defined on its domain and continuous, and that $f_P(g_P(M)) = M$ for all $M \in SO(n)$. In these proofs, we use 0 to denote the zero vector in the appropriate Euclidean space. We also use the same slicing notation from the main paper. That is, if u is a vector of length m , define the slicing notation $u_{i:j} = (u_i, u_{i+1}, \dots, u_j)$, and $u_i = u_{i:m}$.

Proof that g_P is defined on $SO(n)$. Suppose $M \in SO(n)$. The same as we did for Equation (10) in the main paper, define a vectorized representation $\gamma(M)$ by dropping the last column of M : $\gamma(M) = [M_{(1)}^T, \dots, M_{(n-1)}^T]$, where $M_{(i)}$ indicates the i th column of M . Following Equation (8), which defines the *normalized projection*, and Equation (10), let $v = \gamma_{n^2-2n} / \|\gamma_{n^2-2n}\|$. The only way that $g_P(M)$ could not be defined is if the normalized projection $P(v)$ is not defined, which requires $v_1 = 1$. However, if $v_1 = 1$, then because v is unit length, it follows that

γ_{n^2-2n+1} : has length zero. But γ_{n^2-2n+1} : is a column vector from $M \in SO(n)$, and therefore has unit length. We conclude that $v_1 \neq 1$ and g_P is defined on $SO(n)$.

Proof that g_P is continuous. This case is trivial because g_P is the composition of functions that are continuous on their domains and thus is also continuous on its domain.

Lemma 1. We claim that if $u \in \mathbb{R}^m$ and $\|u_2\| = 1$, then $Q(P(u)) = u$. We now prove this. We have $\|u\| = \sqrt{1 + u_1^2}$. Then we find by Equation (8) that

$$\|P(u)\| = \frac{1}{\|u\| - u_1} = \frac{1}{\sqrt{1 + u_1^2} - u_1} \quad (17)$$

Now let $b = Q(P(u))$. Components 2 through m of b are $P(u)/\|P(u)\|$, but this is just u_2 . Next, consider b_1 , the first component of b :

$$b_1 = \frac{1}{2} \left[\|P(u)\| - \frac{1}{\|P(u)\|} \right] \quad (18)$$

$$= \frac{1}{2} \left[\frac{1 - (1 + u_1^2) + 2\sqrt{1 + u_1^2}u_1 - u_1^2}{\sqrt{1 + u_1^2} - u_1} \right] \quad (19)$$

$$= u_1 \quad (20)$$

We find that $b = u$, so $Q(P(u)) = u$.

Proof that $f_P(g_P(M)) = M$ for all $M \in SO(n)$. For the term $f_{GS}(A)$ of Equation (11), this is defined on $\mathbb{R}^{n(n-1)} \setminus D$. Here A is the matrix argument to f_{GS} in Equation (11), and D is the set where the dimension of the span of A is less than $n - 1$. Let $M \in SO(n)$. The same as before, let $\gamma(M)$ be the vectorized representation of M , which drops the last column. By Lemma 1, $Q(P(\gamma_{n^2-2n})) = \gamma_{n^2-2n}$. Thus by Equation (11), we have $f_P(g_P(M)) = f_{GS}(\gamma^{(n \times n-1)}) = f_{GS}(g_{GS}(M)) = M$.

D. The Unit Quaternions are a Discontinuous Representation for the 3D Rotations

In Case 2 of Section 4, we showed that the quaternions are not a continuous representation for the 3D rotations. We intentionally used a simpler formulation for the quaternions, which is easier to understand and also saves space in the paper, due to its quaternions in general not being unit length. However, an attentive reader might wonder what happens if we use the unit quaternions: is the discontinuity removable? However, we show here that the unit quaternions are also not a continuous representation for the 3D rotations.

We use a mapping g_u to map $SO(3)$ to the unit quaternions, which we consider as the Euclidean space \mathbb{R}^4 . We use the formula by [2, 5]:

$$g_u(M) = \left[\begin{array}{c} \text{copysign}(\frac{1}{2}\sqrt{1+M_{11}-M_{22}-M_{33}}, M_{32}-M_{23}) \\ \text{copysign}(\frac{1}{2}\sqrt{1-M_{11}+M_{22}-M_{33}}, M_{13}-M_{31}) \\ \text{copysign}(\frac{1}{2}\sqrt{1-M_{11}-M_{22}+M_{33}}, M_{21}-M_{12}) \\ \frac{1}{2}\sqrt{1+M_{11}+M_{22}+M_{33}} \end{array} \right] \quad (21)$$

Here $\text{copysign}(a, b) = \text{sgn}(b)|a|$. Now consider the following matrix in $SO(3)$, which is parameterized by θ :

$$B(\theta) = \begin{bmatrix} \cos(\theta) & -\sin(\theta) & 0 \\ \sin(\theta) & \cos(\theta) & 0 \\ 0 & 0 & 1 \end{bmatrix}. \quad (22)$$

By substitution, we can find the components of $g_u(B(\theta))$ as a function of θ . For example, as $\theta \rightarrow \pi^-$, the third component is $\sqrt{(1 - \cos(\theta))/2} = 1$. Meanwhile, as $\theta \rightarrow \pi^+$, the third component is $-\sqrt{(1 - \cos(\theta))/2} = -1$. We conclude that the unit quaternions are not a continuous representation.

A similar representation is the Cayley transformation [1] which has a different scaling to the unit quaternion, where $w = 1$ and the vector (x, y, z) is the unit axis of rotation scaled by $\tan(\theta/2)$. The limit goes to infinity when approaching 180° . Thus, it is not a representation for $SO(3)$.

E. Interaction Between 5D and 6D Continuous Representations and Discontinuous Ones

In some cases, it may be convenient to use a common 3D or 4D angle representation, such as the quaternions or Euler angles. For example, the quaternions may be useful when interpolating between two rotations in $SO(3)$, or when there is an existing neural network that already accepts quaternion inputs. However, as we showed in the main paper Case 2 of Section 4.1, all 3D and 4D representations for rotations are discontinuous.

One solution for the above conundrum is to simply convert as needed from the continuous 5D and 6D representations that we presented in Case 3 and 4 of Section 4.2 to the desired representation. For concreteness, suppose the desired representation is the quaternions. Assume that any conversions done in the network are only in the direction that maps to the quaternions. Then the associated mapping in the opposite direction (i.e. from quaternions to the 5D or 6D representation) is continuous. If losses are applied only at points in the network where the representation is continuous (e.g. on the 5D or 6D representations), then the learning should not suffer from discontinuity problems. One can convert from the 5D or 6D representation to quaternions by first applying Equation (5) or Equation (10) and then using Equation (4). Of course, one could also make a similar argument for other discontinuous but popular angle representations such as Euler angles.

F. Visualizing Discontinuities in 3D Rotations

Here we visualize any discontinuities that might occur in the 3D rotation representations. We do this by forming three continuous curves in $SO(3)$, which we call the “X, Y, and Z Rotations.” We map each of these curves to each representation, and then map the representation curve to 2D by retaining the top two components from Principal Components Analysis (PCA). We call the first curve in $SO(3)$ the “X Rotations:” this curve is formed by taking the X axis $(1, 0, 0)$, and constructing a curve consisting of all rotations around

this axis as parameterized by angle. Likewise, we call the second and third curves in $SO(3)$ the “Y Rotations” and “Z Rotations:” these curves are formed by rotating around the Y and Z axes, respectively. We show the resulting 2D curves in Figure 6.

G. Additional Empirical Results

In this section, we show some additional empirical results.

G.1. Visualization of Inverse Kinematics Test Result

In Figure 7, we visualize the worst two frames with the highest pose errors generated by the network trained on quaternions, along with the corresponding results from the network trained with 6D representations. Likewise, we show the two frames with highest pose errors generated by the network trained on our 6D representation, along with the corresponding results from the network trained on quaternions. This shows that for the worst error frames, the quaternion representation introduces bad qualitative results while the 6D one still creates a pose that is reasonable.

G.2. Additional Sanity test

In the main paper, Section 5.1, we show the sanity test result of the network trained with L2 loss between the ground-truth and the output rotation matrices. Another option for training is using the geodesic loss. Besides, the networks in the main paper are trained and tested using a uniform sampling of the axis and the angle which is not a uniform sampling on $SO(3)$ [26]. We present the sanity test result of using the geodesic loss and the two sampling methods in Figure 8. They are both similar to the result in the main paper.

Additional representations. In addition to common rotation representations like Euler angles, axis-angles and quaternions, we investigated a few other rotation representations used in recent work including a 3D Rodriguez vector representation, and quaternions that are constrained to one hemisphere as given by Kendall et al. [20]. The 3D Rodriguez vector is given as $R = \omega\theta$, where ω is a 3D unit vector and θ is the angle [7]. We will not provide the proofs for the discontinuity in these representations, but we show their empirical results in Figure 8. We find that the errors are significantly worse than our 5D and 6D representations.

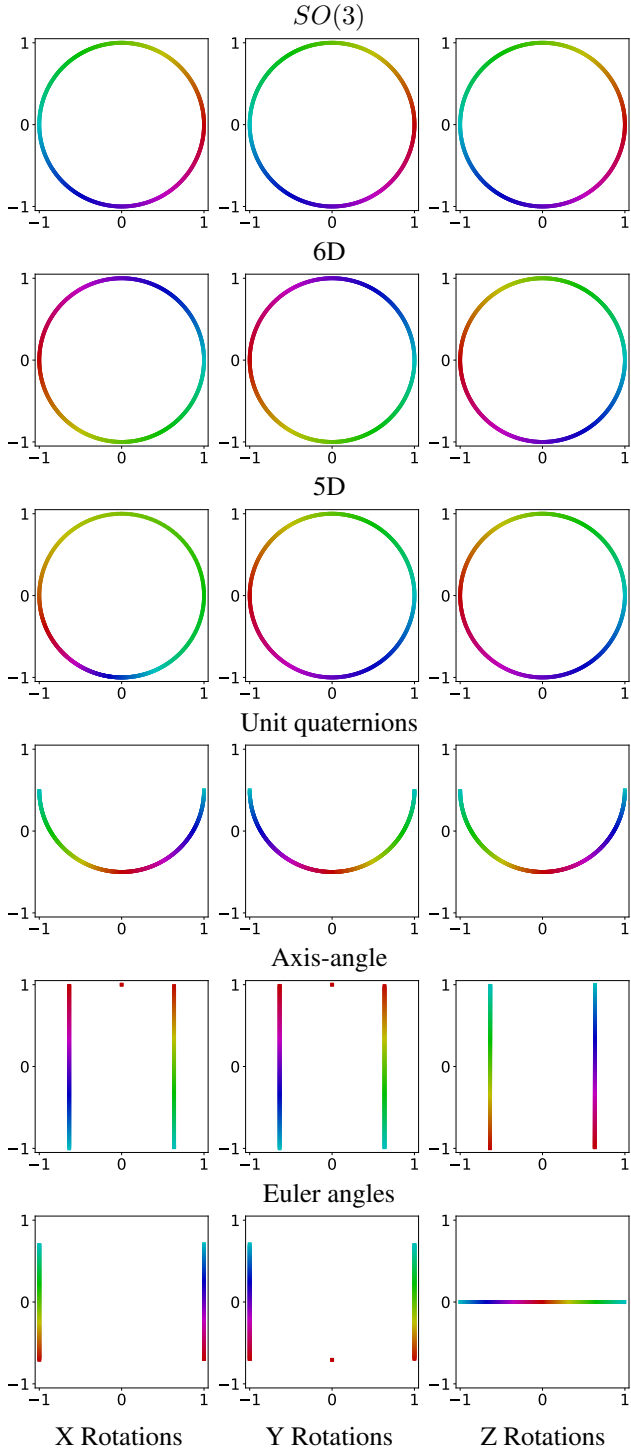
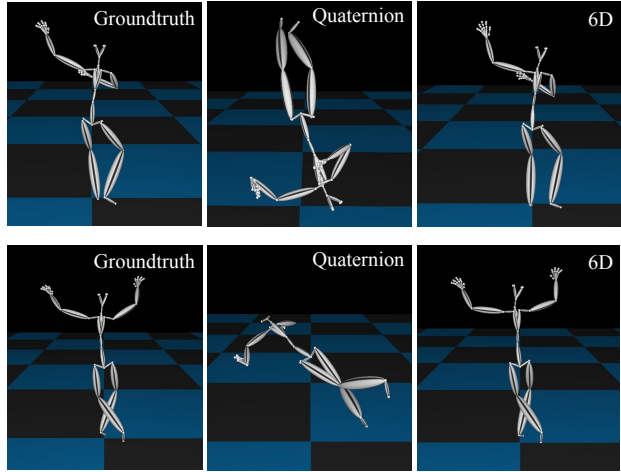


Figure 6. Visualization of discontinuities in 3D rotation representations. In the three columns, we show three different curves in $SO(3)$: the “X, Y, and Z Rotations,” which consist of all rotations around the corresponding axis. We map each curve in $SO(3)$ to each of the rotation representations in the different rows (plus the top row, which stays in the original space $SO(3)$), and then map to 2D using PCA. We use the hue to visualize the rotation angle in $SO(3)$ around each of the three canonical axes X, Y, Z. If the representation is continuous then the curve in 2D should be homeomorphic to a circle, and similar colors should be nearby spatially. We can clearly see that the topology is incorrect for the unit quaternion, axis-angle, and Euler angle representations.

Worst Two Frames using Quaternion



Worst Two Frames using the 6D representation

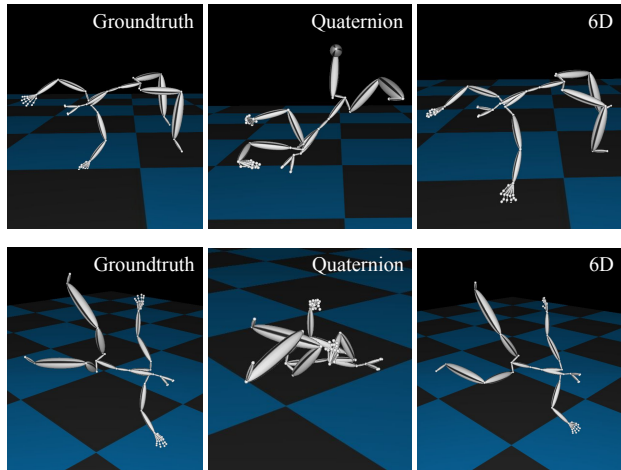
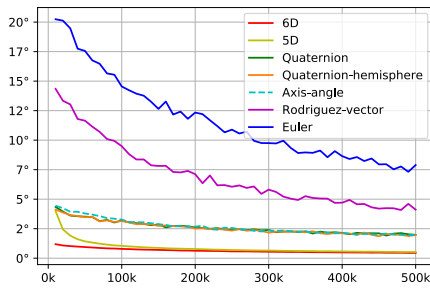
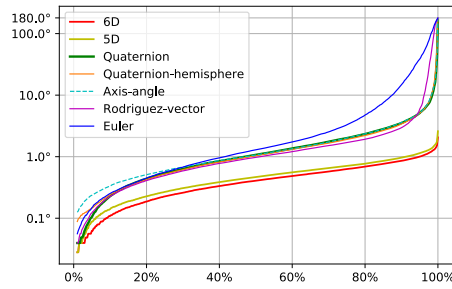


Figure 7. At top, we show IK results for the two frames with highest pose error from the test set for the network trained using quaternions, and the corresponding results on the same frames for the network trained on the 6D representation. At bottom, we show the two worst frames for the 6D representation network, and the corresponding results for the quaternion network.

Sanity Test – Geodesic Loss and Uniform Sampling on Axis and Angle



a. Mean errors during iterations.

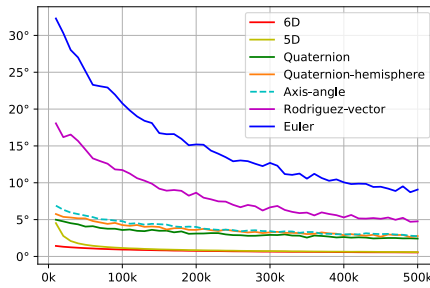


b. Percentile of errors at 500k iteration.

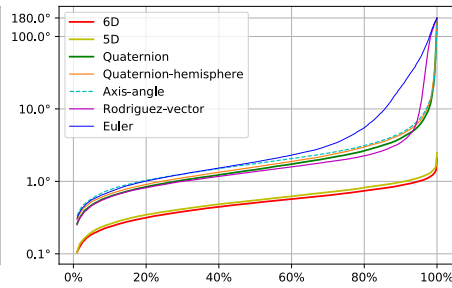
	Mean(°)	Max(°)	Std(°)
6D	0.45	2.33	0.29
5D	0.52	3.19	0.33
Quat	2.02	180.0	6.08
Quat-hemi	3.47	179.22	6.72
AxisA	2.0	179.58	5.43
Euler	7.45	179.87	21.87
Rodriguez	4.17	180.0	17.78

c. Errors at 500k iteration.

Sanity Test – Geodesic Loss and Uniform Sampling on SO(3)



d. Mean errors during iterations.



e. Percentile of errors at 500k iteration.

	Mean(°)	Max(°)	Std(°)
6D	0.54	1.82	0.26
5D	0.59	1.93	0.29
Quat	2.4	176.9	6.81
Quat-hemi	2.72	179.55	7.03
AxisA	2.89	175.53	6.77
Euler	9.12	179.93	24.01
Rodriguez	4.74	179.45	17.84

f. Errors at 500k iteration.

Figure 8. Additional Sanity test results. “Quat” refers to quaternions, “Quat-hemi” refers to quaternions constrained to one hemisphere[20], “AxisA” refers to axis angle and “Rodriguez” refers to the 3D Rodriguez-vector.